



Research paper

Synthesis of a novel ZnO nanoplates supported hydrazone-based palladacycle as an effective and recyclable heterogeneous catalyst for the Mizoroki-Heck cross-coupling reaction



Fatemeh Nouri, Shahnaz Rostamizadeh*, Mohammad Azad

Department of Chemistry, K.N. Toosi University of Technology, P.O. Box: 15875-4416, Tehran, Iran

ARTICLE INFO

Article history:

Received 27 September 2017

Received in revised form 27 November 2017

Accepted 28 November 2017

Available online 2 December 2017

Keywords:

Palladacycle

Heterogeneous catalyst

ZnO nanoplates

Mizoroki-Heck cross-coupling

ABSTRACT

A new hydrazone-based palladacycle complex was successfully prepared onto ZnO nanoplates support and was fully identified by using a variety of methods such as energy dispersive X-ray spectroscopy (EDX), Brunauer-Emmett-Teller analysis (BET), inductively coupled plasma technique (ICP), thermogravimetric analysis (TGA), Fourier transform infrared spectroscopy (FT-IR) and X-ray photoelectron spectroscopy (XPS). The morphology of nanoplates support has been also confirmed by scanning electron microscopy (SEM) and powder X-ray diffraction (XRD). Furthermore, it was shown that ZnO nanoplates supported hydrazone-based palladacycle can act as a highly efficient heterogeneous catalyst for the Mizoroki-Heck cross-coupling reaction with excellent yields. The reaction was successfully carried out between aryl iodides, bromides or even aryl chlorides with a variety of olefins. Additionally, it is possible to isolate the catalyst from the reaction mixture and reused for eight sequential cycles without remarkable decrease in catalytic activity.

© 2017 Elsevier B.V. All rights reserved.

1. Introduction

Palladium-catalyzed processes facilitate the formation of C–C bonds between aryl halides and vinyl groups via Mizoroki-Heck type reactions, which provide a versatile, effective and common way for the synthesis of various substituted olefins [1–3]. Therefore, palladium-catalyzed reactions accelerate the organic synthetic routes into a large number of biological and medicinal compounds [4–6]. However, in most of the reactions catalyzed by palladium complexes, in addition to low catalytic efficiency, a catalyst with high loading amount of Pd and an inert atmosphere are commonly required to promote the conversion, which is costly and not suitable from an environmental viewpoint [7]. Thus, utilization of the new palladium complexes as catalyst has been of considerable interest especially regarding aryl chlorides [8–10] under aerobic and aqueous conditions [11–14]. In the past few years, various Pd(II) complexes, such as *N*-heterocyclic carbene [15] and phospho-containing complexes [16] have been applied as catalyst in C–C cross-coupling reactions. In addition, YCY-type [17] and CY-type palladacycles [18,19], in which Y could be various functional groups bound to palladium through P, N, S or O atoms, have also demonstrated their catalytic activities [20,21].

However, palladacycles are known to be the most efficient catalysts among the other Pd(II) complexes [22,23]; and between the several types of palladacycle catalysts, CN-type palladacycles, which exist typically as bridged dimers by halogen or acetate, are one of the most effective palladium catalysts for carbon-carbon bond formation due to having a highly energetic C–Pd bond [24,25], in which the nitrogen atom can be from amine [26,27], imine [28,29], oxime [30], hydrazone [31] or *N*-heterocycle ligands and etc. Also, the metalated carbon is usually an aromatic sp² carbon. For example, Iyer reported the cyclopalladated acetylferrocenyl oxime as a CN-type palladacycle in the Mizoroki-Heck coupling reaction [32]. Nowtony [33] and Wu [34] also investigated the use of imino-palladacycle complexes in this type of C–C coupling reaction in good yields.

Although, the palladacycle catalysts as Herrmann described, are effectively able to promote many reactions, similar to Heck coupling reaction [35], these catalysts suffer from some disadvantages associated with their instability, the necessity of using toxic phosphine auxiliary ligands, degradation, deactivation of catalyst during the first run as well as palladium leaching and difficult separation [36]. However, to the extent of our knowledge, a little research on the stability, recovery and reusability of these catalysts has been performed in the literature. In recent years, efforts have been made to solve the problem by immobilization of palladacycles on different supports. Accordingly, Nowotny et al. immobilized

* Corresponding author.

E-mail address: shrostamizadeh@yahoo.com (S. Rostamizadeh).

the previously synthesized imine-based palladacycle complex onto polystyrene to improve its reusability for the Heck reaction. However, it failed after the second run [33]. As a result, a phospho-containing ligand was used for the recovery of the Pd catalysts during the reaction [37–42]. Afterwards, Gladysz prepared an imine-type palladacycle immobilized onto a thermomorphic fluororous polymer, in which recyclability of the catalyst was enhanced significantly; but this reactivity was not observed for aryl bromides [43]. Moreover, Alonso et al. used the graphene oxide supported oxime-palladacycle in the coupling reaction, in which the efficiency of the catalyst was missed in third run [44]. In this manner, some palladacycles were immobilized onto polystyrene [45–48], chitosan [49], polyethylene glycol [50], Fe₃O₄ nanoparticles [51], MCM-41, SiO₂, polystyrene-divinyl benzene polymer [52] and polyvinyl pyridine [53] supports to obtain an improved heterogeneous catalyst. But these catalysts have still been suffering from the problem of low reusability and low catalytic activity, especially for aryl bromides and chlorides. Therefore, the exploration of new stable palladacycles is still required. To the best of our knowledge, no research dealing with immobilization of a palladacycle onto ZnO support has been reported. ZnO is a valuable material in biomedicine, ceramics, ointments, foods, etc. [54] due to its exceptional physical and chemical properties including high chemical, thermal and mechanical stability [55], hardness, biocompatibility and biodegradability, antibacterial and non-toxicity [56–58]. Furthermore, ZnO nanoparticles, by having high surface area to volume ratio and considerable stability as mentioned above, are expected to be an efficient, suitable, and stable heterogeneous support for organic catalytic centres [59–62]. Therefore, in continuation of our research interest in preparing of heterogeneous nano catalysts [63–66], we are intending to prepare a new hydrazone-based palladacycle which can be immobilized onto ZnO nano support to promote its stability and catalytic activity. To do so, we chose a hydrazone ligand containing carboxylate groups; because carboxylate anions strongly adsorb Zn centres and significantly adjust the surface morphologies by promoting or reducing the crystal growth as well [67–70]. Although, organic additives have been widely used to alter the crystal growth of ZnO nanoparticles, but this strategy has not been used for immobilization of organometallic catalytic centres onto ZnO nanostructure support.

Herein, for the first time, we report the synthesis of a novel ZnO nanoplates supported hydrazone-based palladacycle which can be applied as a highly effective and reusable palladacycle catalyst for running Mizoroki-Heck cross-coupling reaction between aryl halides and various olefins with high yields in short reaction times even for aryl chlorides.

2. Experimental

2.1. Materials and instruments

All chemical materials were supplied from Aldrich, Merck and Fluka. A Buchi or Heidolph rotary evaporator was employed to remove solvents at reduced pressure. Thin layer chromatography plate was prepared on plates of silica gel 60 (5–40 μm mesh size diameter) on glass plates (20 × 20 cm²) using 10 g of silica gel. IR spectroscopy was accomplished by a Shimadzu FTIR-8300 spectrophotometer. ¹H and ¹³C NMR of the resulting Mizoroki-Heck products were provided with Bruker Avance spectrometer at 300 and 75 MHz, respectively. Inductively coupled plasma technique was performed by Varian Vista-MPX instrument to determine the amount of metal. Thermogravimetric curve was recorded under nitrogen atmosphere by NETZSCH STA 409 PC instrument. Energy dispersive X-ray analysis was achieved using Vega TESCAN-Model scanning electron microscope supplied with energy dispersive

X-ray equipment. X-ray diffraction was performed using a PHILIPS X-ray diffractometer system (PW1800-Model). The surface morphology of the ZnO nanoplates supported hydrazone-based palladacycle catalyst was analysed by scanning electron microscope (KYKY-EM3200 Digital Scanning). A 2400 series II PerkinElmer elemental analyzer was employed for the CHN analysis. A twin anode X-ray source system (XR3E2, 8025-BesTec) was applied for X-ray photoelectron spectroscopy analysis. The specific surface area of the nanostructure was determined by the nitrogen sorption measurement, ([5.0.0.3] Belsorp, BEL Japan, INC.). The porous structural parameter in this paper is based on Barret-Joyner-Halenda (BJH) data. The NMR spectra of the products in Table 5 were provided with electronic Supplementary information (ESI).

2.2. Synthesis of the catalyst

2.2.1. Synthesis of hydrazone ligand (1)

4-formylbenzoic acid (0.300 g, 2 mmol) was dissolved in dry MeOH (20 mL) at room temperature and then hydrazine hydrate·6H₂O (0.1 mL, excess) was added dropwise to the solution according to the literature procedure with slightly modification [71]. After a few minutes yellow crystals precipitated. The product was collected by filtration, washed with MeOH and acetonitrile, and then dried under vacuum condition. As a result, the compound (1E,2E)-1,2-bis(1,4-hydrazinumbenzoyl)ethyldiene) hydrazone was synthesized as yellow fine powder (0.3 g, 95%). δH (300 MHz; [D6] DMSO; Me₄Si): 7.07 (10H, br s, NH₂-NH₃⁺), 7.57 (3J = 8.9, 4H, d, CH), 7.82 (3J = 8.9, 4H, d, CH), 8.66 (2H, s, CH = N); δC (75 MHz; [D6] DMSO; Me₄Si): 129.9 (CH), 130.0 (CH), 139.0 (C), 140.0 (C), 162.4 (C = N), 172.4 (COO⁻). Also, elemental analysis was performed to confirm the synthesis of the ligand (Found: C, 53.3; H, 5.1; N 22.7. Calc. for C₁₆H₂₀N₆O₄: C, 53.3; H, 5.5; N, 23.3%).

2.2.2. Synthesis of ZnO nanoplates supported hydrazone ligand (hydrazone@ZnO, 2)

ZnO nanoplates supported hydrazone ligand was synthesized by reacting Zn(NO₃)₂·6H₂O (1.18 g, 4 mmol) with the prepared hydrazone ligand (1) (0.3 g) in 25 mL DMF in a sealed vessel reaction. Then the yellow solution was heated at 90 °C for 18 h. As soon as the solution temperature reached to 90 °C, ZnO nanoplates hydrazone ligand rapidly was produced from solution. After 18 h, the resulting pale yellow powder was collected by filtration, washed with DMF and subsequently with chloroform and dried under vacuum for 2 h to give ZnO nanoplates supported hydrazone ligand (2).

2.2.3. Synthesis of ZnO nanoplates supported hydrazone-based palladacycle catalyst (hydrazone-Pd@ZnO, 3)

To 0.3 g ZnO nanoplates supported hydrazone ligand was added 0.045 g Pd(OAc)₂ and 100 mL dry dichloromethane as solvent. The lemon mixture was stirred at room temperature for 1 day. Subsequently, the cream-green mixture was centrifuged and washed several times with dichloromethane and allowed to dry at 80 °C.

2.3. General procedure for Mizoroki-Heck coupling reaction of aryl halides with olefins

To a 25 mL round bottom flask containing aryl halide (1 mmol), olefin (1.2 mmol), Et₃N (1.5 mmol), and ZnO nanoplates supported hydrazone-based palladacycle (10 mg, 0.26 mol% Pd), 3 mL DMF was added as solvent. The resulting solution was stirred at 130 °C in an oil bath. The reaction was followed by TLC (thin layer chromatography) and at the end; it was allowed to cool to room temperature and was centrifuged to separate the catalyst. The residue was diluted with ethyl acetate (2 × 5 mL), and washed with water (2 × 5 mL). Then the organic phase was dried with

anhydrous MgSO₄, filtered, and the solvent was removed by evaporation under vacuum conditions. Further purification was achieved by thin layer chromatography plate, using EtOAc and n-hexane with 2:10 ratio as eluent.

2.3.1. Selected spectral data of the Mizoroki-Heck products

2.3.1.1. (*E*)-4-styrylbenzotrile (6a, 6g). δ H (300 MHz; CDCl₃; Me₄Si): 7.09 (³J = 18.25, 1H, d, CH), 7.22 (³J = 18.25, 1H, d, CH), 7.32 (1H, dd, CH), 7.39 (2H, dd, CH), 7.54 (³J = 8.2, 2H, d, CH), 7.57 (³J = 7.4, 2H, d, CH), 7.64 (³J = 7.4, 2H, d, CH); δ C (75 MHz; CDCl₃; Me₄Si): 110.5, 119.03, 126.7, 126.8, 126.9, 128.6, 128.8, 132.4, 132.4, 136.2, 141.8.

2.3.1.2. (*E*)-1-methyl-4-styrylbenzene (6b, 6l). δ H (300 MHz; CDCl₃; Me₄Si): 2.39 (3H, s, CH₃), 7.04 (³J = 18.49, 1H, d, CH), 7.17 (³J = 18.49, 1H, d, CH), 7.22 (³J = 8.8, 2H, d, CH), 7.27 (1H, dd, CH), 7.38 (2H, dd, CH), 7.44 (³J = 8.9, 2H, d, CH), 7.54 (³J = 8.8, 2H, d, CH); δ C (75 MHz; CDCl₃; Me₄Si): 21.2, 126.4, 126.4, 128.6, 128.6, 127.4, 127.7, 129.4, 134.5, 137.5, 137.5.

2.3.1.3. (*E*)-1-(4-styrylphenyl)ethanone (6c). δ H (300 MHz; CDCl₃; Me₄Si): 2.60 (3H, s, CH₃), 7.12 (³J = 18.15, 1H, d, CH), 7.22 (³J = 18.15, 1H, d, CH), 7.30 (1H, dd, CH), 7.39 (2H, dd, CH), 7.54 (³J = 8.1, 2H, d, CH), 7.58 (³J = 9.2, 2H, d, CH), 7.95 (³J = 9.2, 2H, d, CH); δ C (75 MHz; CDCl₃; Me₄Si): 26.6, 126.4, 126.8, 127.4, 128.3, 128.8, 128.8, 131.4, 135.9, 136.6, 141.9, 197.4.

2.3.1.4. (*E*)-3-*p*-tolylacrylonitrile (6d). δ H (300 MHz, CDCl₃; Me₄Si): 2.38 (3H, s, CH₃), 5.80 (³J = 18.51, 1H, d, CH), 7.20 (³J = 9.0, 2H, d, CH), 7.33 (³J = 9.0, 2H, d, CH), 7.34 (³J = 18.51, 1H, d, CH); δ C (75 MHz; CDCl₃; Me₄Si): 21.5, 94.9, 118.4, 127.3, 129.8, 130.8, 141.8, 150.5.

2.3.1.5. (*E*)-3-(4-acetylphenyl)acrylonitrile (6e). δ H (300 MHz, CDCl₃; Me₄Si): 2.64 (3H, s, CH₃), 5.83 (³J = 18.54, 1H, d, CH), 7.15 (³J = 18.54, 1H, d, CH), 7.31 (³J = 9.3, 2H, d, CH), 7.64 (³J = 9.3, 2H, d, CH); δ C (75 MHz; CDCl₃; Me₄Si): 30.9, 98.7, 117.5, 127.4, 128.6, 137.3, 138.2, 148.8, 196.9.

2.3.1.6. (*E*)-1-methoxy-3-styrylbenzene (6i). δ H (300 MHz; CDCl₃; Me₄Si): 3.86 (3H, s, CH₃), 6.83 (³J = 16.7, 1H, d, CH), 7.10 (4H, m, CH), 7.26 (1H, s, CH), 7.28 (1H, dd, CH), 7.38 (2H, dd, CH), 7.52 (³J = 8.1, 2H, d, CH); δ C (75 MHz; CDCl₃; Me₄Si): 55.5, 111.7, 113.2, 119.2, 126.5, 127.6, 128.5, 128.6, 129.0, 129.6, 137.2, 138.7, 159.8.

2.3.1.7. (*E*)-*n*-butyl 3-*p*-tolylacrylate (6j). δ H (300 MHz; CDCl₃; Me₄Si): 0.97 (3H, t, CH₃), 1.44 (2H, m, CH₂), 1.69 (2H, m, CH₂), 2.37 (3H, s, CH₃), 4.20 (2H, t, CH₂), 6.39 (³J = 17.7, 1H, d, CH), 7.18 (³J = 8.9, 2H, d, CH), 7.42 (³J = 8.9, 2H, d, CH), 7.66 (³J = 17.7, 1H, d, CH); δ C (75 MHz; CDCl₃; Me₄Si): 13.7, 19.2, 21.4, 30.7, 64.3, 117.1, 128.0, 129.5, 131.7, 140.5, 144.5, 167.2.

2.3.1.8. (*E*)-*n*-butyl 3-(4-acetylphenyl)acrylate (6k). δ H (300 MHz, CDCl₃; Me₄Si): 0.96 (3H, t, CH₃), 1.44 (2H, m, CH₂), 1.69 (2H, m, CH₂), 2.60 (3H, s, CH₃), 4.22 (2H, t, CH₂), 6.52 (³J = 17.8, 1H, d, CH), 7.59 (³J = 9.2, 2H, d, CH), 7.68 (³J = 17.8, 1H, d, CH), 7.96 (³J = 9.2, 2H, d, CH); δ C (75 MHz; CDCl₃; Me₄Si): 14.0, 19.1, 22.6, 31.9, 64.6, 120.8, 128.0, 128.4, 137.9, 138.7, 142.9, 166.5, 197.1.

2.3.1.9. (*E*)-1,2-diphenylethene (6n, 6o). δ H (300 MHz, CDCl₃; Me₄Si): 7.13 (1H, s, CH), 7.28 (1H, dd, CH), 7.38 (2H, dd, CH), 7.54 (2H, d, CH); δ C (75 MHz; CDCl₃; Me₄Si): 126.5, 127.6, 127.9, 128.6, 137.3.

2.3.1.10. (*E*)-*n*-butyl 3-*m*-tolylacrylate (6r). δ H (300 MHz, CDCl₃; Me₄Si): 0.98 (3H, t, CH₃), 1.45 (2H, m, CH₂), 1.71 (2H, m, CH₂), 2.38 (3H, s, CH₃), 4.22 (2H, t, CH₂), 6.44 (³J = 17.7, 1H, d, CH), 7.20 (³J = 8.2, 1H, d, CH), 7.27 (1H, m, CH), 7.33 (2H, m, CH), 7.67 (³J = 17.7, 1H, d, CH); δ C (75 MHz; CDCl₃; Me₄Si): 13.7, 19.2, 21.2, 30.1, 64.3, 118.0, 123.9, 125.2, 128.7, 130.9, 134.4, 138.4, 144.7, 168.0.

3. Results and discussion

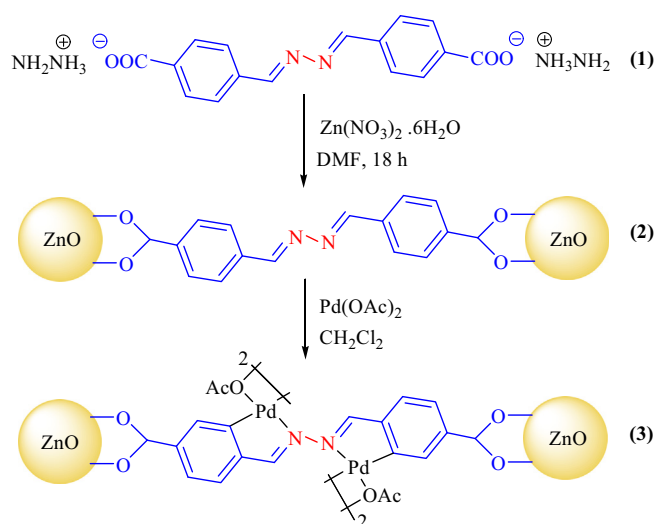
3.1. Preparation and characterization of the catalyst

All the steps involved in the preparation of the catalyst have been outlined in Scheme 1. As shown in Scheme, we firstly prepared a hydrazone ligand (**1**) and then immobilized it onto ZnO nanoplates support (**2**). Finally, by insertion of palladium, the heterogeneous ZnO nanoplates supported hydrazone-based palladacycle catalyst (**3**) was successfully produced.

The presence of corresponding functional groups at different steps was confirmed by FTIR analysis (given at ESI). In IR spectra of ligand (**1**), the medium peak appeared at 959 cm⁻¹ and two sharp peaks at 1378 and 1617 cm⁻¹ are related to the N–N bond in hydrazone functional group, symmetric and asymmetric stretching vibrations in carboxylate ions, respectively. Also, the Zn–O bond stretching appeared at 431 cm⁻¹ and C=N vibration band was observed at 1657 cm⁻¹ for free ligand in IR spectra of compound (**2**). After the cyclopalladation, in IR spectra of catalyst (**3**), the C=N band shifted to lower frequency 1646 cm⁻¹ and a new small peak appeared at 1412 cm⁻¹ could be assigned to C–O stretching vibration of the acetate bound to Pd [72].

Moreover, in order to determine all the elements, the synthesized compound (**2**) was characterized by energy-dispersive X-ray spectroscopy (EDX) (Fig. 1a). The presence of palladium in the catalyst (**3**) was confirmed by EDX as well (Fig. 1b). As seen in Fig. 1, the obtained ZnO supported hydrazone-based palladacycle contains all the elements in both of the organic ligand and the ZnO nanostructure as support.

Furthermore, according to the inductively coupled plasma-atomic emission spectroscopy (ICP-AES) and elemental analysis shown in Table 1, about 38.18 wt% of the catalyst constructed from Zinc as support and 28.68 wt% carbon as organic ligand. In addition, the amount of palladium incorporated into the ZnO



Scheme 1. Synthesis of ZnO nanoplates supported hydrazone-based palladacycle catalyst.

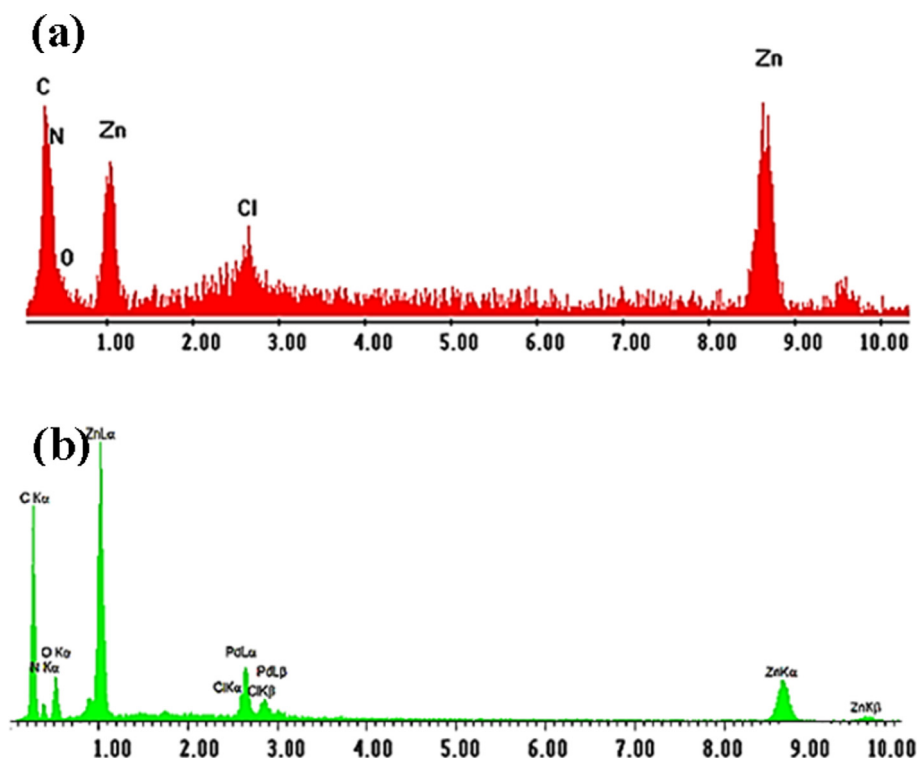


Fig. 1. EDX data of ZnO nanoplates supported hydrazone ligand (2) (a) and ZnO nanoplates supported hydrazone-based palladacycle (3) (b).

Table 1

ICP and elemental analysis of ZnO supported composites.

| Entry | Composite | C% | H% | N% | Zn% | Pd% |
|-------|------------------|-------|------|------|-------|-----|
| 1 | Hydrazone@ZnO | 29.45 | 1.53 | 4.29 | 40.13 | – |
| 2 | Hydrazone-Pd@ZnO | 28.68 | 1.51 | 4.08 | 38.18 | 2.8 |

nano-plates supported hydrazone ligand was also determined by ICP technique. According to this analysis, 2.8 wt% of the Pd was immobilized into the ZnO nanoplates supported hydrazone-based palladacycle, which indicates the synthesized hydrazone ligand, has good capability of binding to the palladium (Table 1).

The XRD patterns of ZnO nanoplates supported hydrazone ligand (2) confirm the formation of the ZnO nanoplates (Fig. 2), in which the crystal phases pattern is remarkably in accordance with Zincite having the wurtzite structure ZnO (JCPDS Card File

No. 36-1451). Moreover, all diffraction peaks are attributed to crystalline phases. The XRD characteristics appeared at 31.56°, 34.24°, 36.08°, 47.32° and 56.51° are due to the diffractions of (1 0 0), (0 0 2), (1 0 1), (1 0 2) and (1 1 0) planes, while the peaks at lower angles 16.56°, 18.40°, 20.14°, 24.84°, 29.48° and 30.81° are related to the organic phase which has been bound as cross-link to ZnO nanoparticles (Fig. 2a). Also, an XRD analysis was performed on ZnO nanoplates supported hydrazone-based palladacycle (3) (Fig. 2b). As seen in Figure, all the peaks were unchanged, which

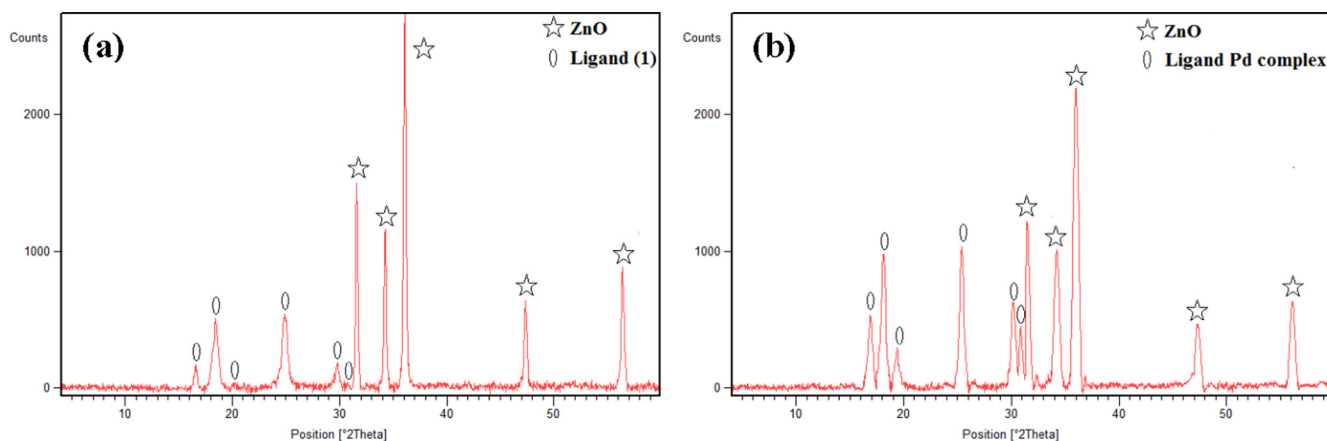


Fig. 2. XRD pattern of ZnO nanoplates supported hydrazone ligand (2) (a) and ZnO nanoplates supported hydrazone-based palladacycle (3) (b).

reveal that the crystalline structure of the compound has been maintained well after palladation and no metallic palladium has been involved [73]. As a result, only palladium complex has been formed.

The morphology of the synthesized ZnO nanostructure supported hydrazone-based palladacycle was characterized from SEM images. As seen in Fig. 3, it could clearly be observed that ZnO nanostructures in the presence of organic ligand containing carboxylate groups resulted in the formation of ZnO nanoplates.

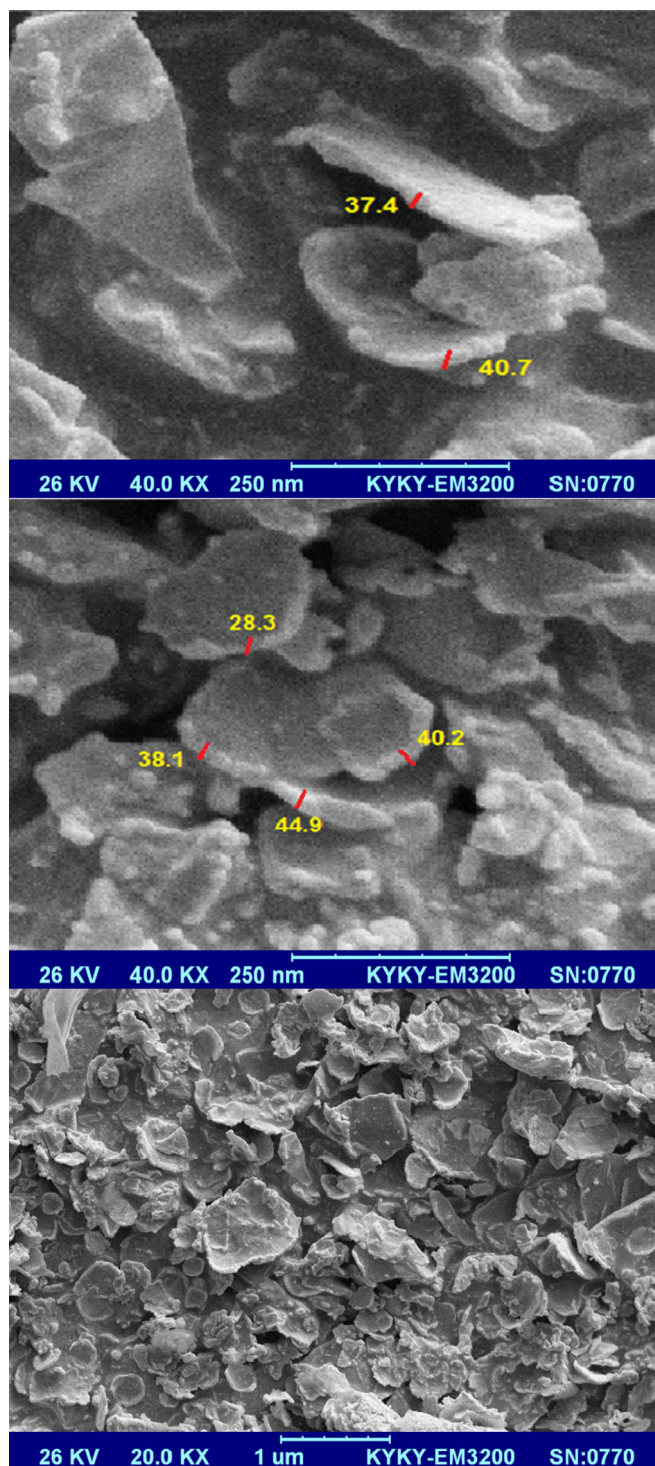


Fig. 3. SEM images of ZnO nanoplates supported hydrazone-based palladacycle (3) catalyst.

The growth of nanoplates is quite typical and is clearly associated to the role of the anionic ligand as cross-linking agent, which restrained the longitudinal growth of nanorods but assisted the growth of plates [67]. Furthermore, as shown in the Fig. 3, thicknesses of nanoplates are about 28–45 nm and their width is between 200 nm and 1000 nm.

In order to investigate the surface area and porous properties of the prepared catalyst (3), the nitrogen adsorption–desorption analysis was performed. The resulting nitrogen adsorption–desorption isotherm and the corresponding BET plot are shown in Fig. 4. Also, the physical parameters including the BET surface area and average pore diameter and pore volume of the ZnO nanostructure supported hydrazone-based palladacycle (3) were summarized in Table 2. The results for catalyst (3), which is a modified ZnO nanoplates with organic moiety, indicate an acceptable surface area in comparison with non-modified ZnO nanoplates, which have surface areas between 3 and 15 m²/g [74–76]. This surface area could be assigned to their small size and thickness. Furthermore, according to the BET experiment in Fig. 4, the sample possess type-III isotherm with a small H3 hysteresis loop according to IUPAC classification [77], which recommends that the pores have a slit and sheet shape [78].

Moreover, the thermal stability of the catalyst was studied by thermogravimetric-differential thermal analysis (TG-DTA) under nitrogen atmosphere (Fig. 5). According to the DTG curve, a slight mass loss occurred below 220 °C which could be related to desolvation or dehydration. In addition, a major mass loss was observed between 220 °C and 550 °C, which was attributed to degradation of the organic materials and the hydrazone-based palladacycle complex. Additionally, the maximum weight loss which has occurred at 380 °C reveals the thermal stability of the catalyst for organic reactions with high temperature.

To investigate the formation of ZnO nanoplates hydrazone-based palladacycle catalyst (3), X-ray photoelectron spectroscopy (XPS) technique was applied. According to this analysis, the presence of C, N, O, Zn and Pd atoms were recognized in the prepared catalyst (Fig. 6). As is clear from Fig. 6b, two evident peaks at 337.60 eV and 343.04 eV are obviously related to 3d_{5/2} and 3d_{3/2} core-levels of Pd(II) in the ZnO nanoplates supported hydrazone-based palladacycle catalyst. The binding energy shifts for Pd(II) 3d_{5/2} of Pd(OAc)₂ from 336.4 eV to 337.6 eV and Pd(II) 3d_{3/2} from 341.7 to 343.0 eV reveals the formation of hydrazone-based palladacycle complex [79]. Also, the XPS spectra of C 1s obviously indicates the peaks at 284.7, 285.0, 286.3 and 288.5 eV, which are related to C=C, C–C, C=N and O–C=O bonds, respectively (Fig. 6c). In addition, the XPS spectra of N 1s in Fig. 6d, clearly exhibits the presence of N=N=C and N–Pd bonds at 400.5 and 402.1 eV [44]. The average peak for O 1s is located at 531.8 eV (Fig. 6e) and the peaks at 90, 1022 and 1044 eV are also related to Zn 3p, 2p_{3/2} and 2p_{1/2}, respectively [80].

3.2. Catalytic application of ZnO nanoplates supported hydrazone-based palladacycle (3) in Mizoroki–Heck cross-coupling reaction

In order to examine the efficiency of the ZnO nanoplates supported hydrazone-based palladacycle catalyst, it was applied in the Mizoroki–Heck cross-coupling reaction. This reaction was chosen, because this type of reactions provides a potent way for the C–C bond formation between olefins and aryl halides in the presence of the palladium complexes. Hence, the optimization of Heck cross-coupling reaction was carried out using 4-bromobenzonitrile (1 mmol) and styrene (1.2 mmol) derivatives in the presence of the ZnO nanoplates supported hydrazone-based palladacycle catalyst (3). The reaction was studied under various conditions such as different amounts of catalyst, different bases, solvents and temperatures. The experimental results are summarized in Tables 3–5. At

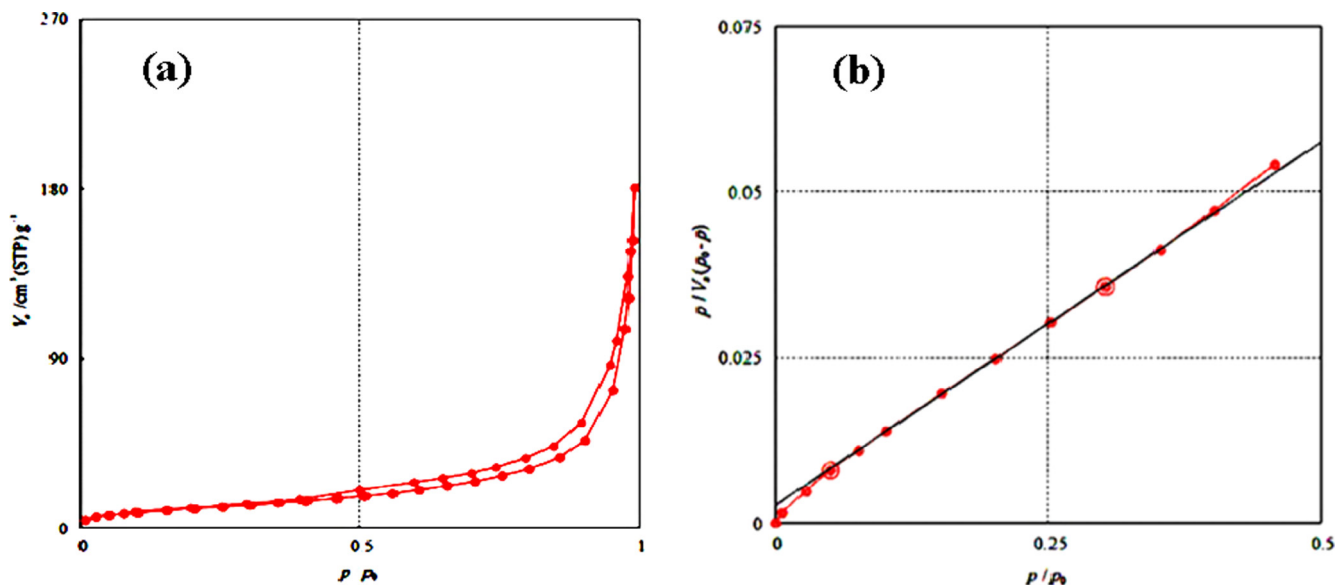


Fig. 4. Nitrogen adsorption-desorption isotherm (a) and BET plot of ZnO nanoplates supported hydrazone-based palladacycle (3) catalyst (b).

Table 2

The results of BET and BJH measurements for ZnO nanoplates supported hydrazone-based palladacycle (3) catalyst.

| Experiment | Results |
|-----------------------------|--|
| BET Surface area | 38.838 (m ² ·g ⁻¹) |
| Average pore diameter | 28.165 (nm) |
| Pore volume | 0.2759 (cm ³ ·g ⁻¹) |
| BJH adsorption surface area | 48.652 (m ² ·g ⁻¹) |

the beginning, the reaction was performed using different amounts of catalyst at 130 °C (Table 3, entries 1–4). As seen in Table, by increasing the amount of catalyst from 0.008 g to 0.010 g, the yield

of the expected product was improved to 95% in a shorter reaction time. But there were no differences in yield and reaction time between 0.010 g (entry 2) and 0.020 g (entry 4) of the catalyst. Therefore, we chose 0.010 g (0.26 mol% Pd) of the catalyst for further experiments. In order to show the unique behaviour of the catalyst, the reaction was also separately examined in the absence of catalyst as well as in the presence of ZnO and ZnO nanoplates supported hydrazone ligand alone (entries 5, 6, 7) in which we did not observe any product even on TLC. Furthermore, a control reaction was also performed in the presence of Pd(OAc)₂ without any ligand and the yield of the reaction was only 20% after 24 h (entry 8) and all of the palladium was also leached into the solution (palladium black), while in the presence of catalyst (3), no palladium black was observed (Section 3.3). The comparison of these

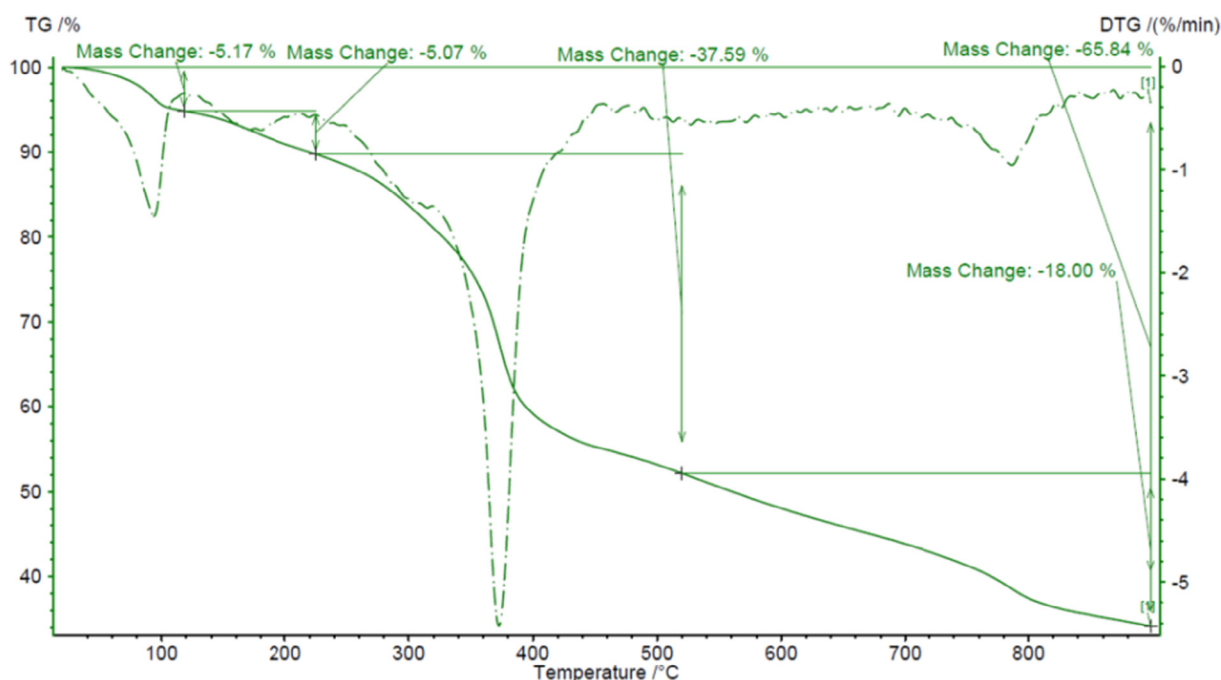


Fig. 5. TG-DTA curve for ZnO nanoplates supported hydrazone-based palladacycle (3).

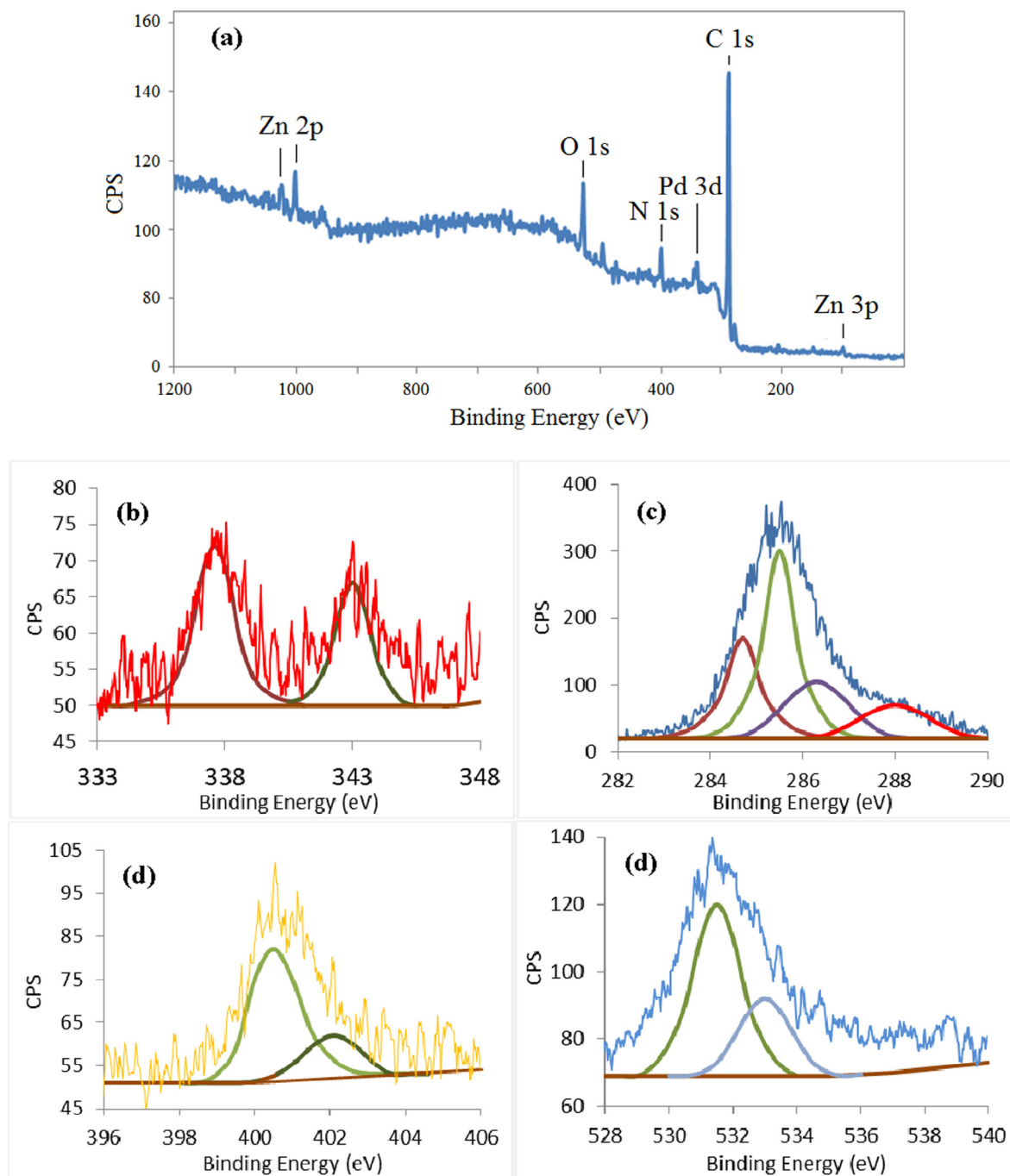


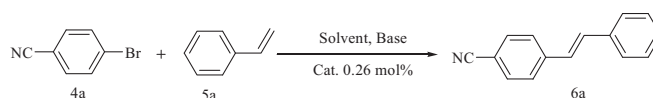
Fig. 6. XPS spectrum: full range (a), the Pd 3d (b), C 1s (c), N 1s (d) and O 1s (e) of the catalyst (**3**).

results showed the stability and catalytic efficiency of the catalyst (**3**) and proved the formation of the hydrazone-based palladacycle complex (**3**). The reaction was then carried out at various temperatures. The comparison of the results in Table 4, entries 6 and 10 revealed that the reaction proceeded slightly better at 130 °C (entry 6). Based on the results outlined in Table 4, it is obvious that Et₃N as organic base acts much better than inorganic bases such as K₂CO₃, Na₂CO₃, and K₃PO₄. Consequently, since Et₃N is an inexpensive and readily available organic base, we chose it for further investigations in the reaction. It is worth mentioning that in the absence of the base only a trace of the product was formed (entry 13). To evaluate the effect of solvent, the reaction was performed in different solvents. The use of DMF/H₂O mixture as solvent in

various ratios produces a by-product (homocoupling) and decreases the reaction yields (Table 4, entries 2, 3). Protic polar solvents, such as EtOH, which was regularly used in coupling reactions catalyzed by Pd, were not operative in the present method (Table 4, entry 7). The use of toluene was not successful and only 30% yield were observed (Table 4, entry 8). Moreover, the reaction progressed much better in DMF (Table 4, entry 1, 4). Then, by adding 0.75 eq TBAB, the reaction time was shortened (Table 4, entry 6), which is due to its ionic environment to stabilize intermediates or transition states in the course of the reaction [81–83]. Therefore, based upon the optimized reaction conditions, the Heck cross-coupling reaction was performed in the presence of the catalyst (**3**) (0.26 mol% Pd), Et₃N and TBAB (was not required for aryl iodides)

Table 3Optimization of the amount of the ZnO nanoplates supported hydrazone-based palladacycle catalyst (**3**) in the Heck reaction^a.

| Entry | Catalyst (g) | mol% of Pd | Time (h) | Yield (%) ^b |
|----------------|----------------------------|------------|----------|------------------------|
| 1 | 0.008 | 0.21 | 2 | 90 |
| 2 | 0.010 | 0.26 | 1 | 95 |
| 3 | 0.015 | 0.39 | 1 | 95 |
| 4 | 0.020 | 0.52 | 1 | 95 |
| 5 | No catalyst | 0 | 24 | 0 |
| 6 | ZnO | 0 | 24 | 0 |
| 7 | Hydrazone@ZnO (2) | 0 | 24 | 0 |
| 8 ^c | Pd(OAc) ₂ | 0.26 | 24 | 20 |

^a Reaction conditions: 4-bromobenzonitrile (1 mmol), styrene (1.2 mmol), Et₃N (1.5 mmol), TBAB (0.75 mmol) in DMF (3 mL) at 130 °C, in the presence of catalyst (**3**) (only entries 1–4).^b Isolated yields.^c Only Pd(OAc)₂ was used as catalyst.**Table 4**Optimization of the reaction conditions for Mizoroki-Heck cross-coupling reaction^a.

| Entry | Solvent | Base | Temperature (°C) | Time (h) | Yield (%) ^b |
|-----------------|----------------------|---------------------------------|------------------|----------|------------------------|
| 1 | DMF | Et ₃ N | 130 | 12 | 65 |
| 2 | DMF/H ₂ O | K ₂ CO ₃ | 130 | 24 | 20 |
| 3 | DMF/H ₂ O | Et ₃ N | 130 | 24 | 30 |
| 4 | DMF | Et ₃ N | 130 | 24 | 85 |
| 5 | DMF | K ₂ CO ₃ | 130 | 36 | 65 |
| 6 ^c | DMF | Et ₃ N | 130 | 1 | 95 |
| 7 ^c | EtOH | Et ₃ N | 80 | 1.5 | 40 |
| 8 ^c | Toluene | Et ₃ N | 110 | 12 | 30 |
| 9 ^c | DMF | Na ₂ CO ₃ | 130 | 1.5 | 20 |
| 10 ^c | DMF | Et ₃ N | 120 | 1 | 90 |
| 11 | DMF | Na ₂ CO ₃ | 130 | 48 | 65 |
| 12 ^c | DMF | K ₃ PO ₄ | 130 | 48 | 72 |
| 13 ^c | DMF | – | 130 | 24 | Trace |

^a Reaction conditions: 4-bromobenzonitrile (1 mmol), styrene (1.2 mmol), base (1.5 mmol) and catalyst (**3**) (0.26 mol%) in solvent (3 mL) in oil bath.^b Isolated yields.^c 0.75 mmol TBAB was added.

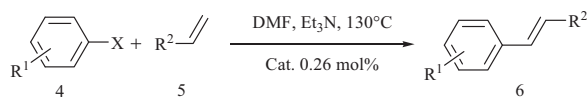
in DMF at 130 °C (entry 6). Finally, in order to show the novelty and generality of the ZnO nanoplates supported hydrazone-based palladacycle catalyst (**3**), we then tried to study the Heck reaction between a range of aryl halides (I, Br and Cl) and different olefins (Table 5). As revealed in Table 5, the reaction of aryl iodides containing electron-rich and electron-poor substituent proceeded easily, and the desired products were achieved with excellent yields. The reaction of aryl bromides was also carried out with high yields. Moreover, derivatives with electron-withdrawing substituents (Table 5, entries 1, 13) were more reactive than those with electron-donating groups (Table 5, entries 8, 9, 17). The steric hindrance caused by the ortho substituents on the aryl halides did not significantly affect the reaction progress, thus 2-bromotoluene proceeded as well as 4-bromotoluene (entries 6, 12). As seen in Table 5, aryl halides with electron-donating substituents at para position such as 4-bromoanisole which have resonance effect, needed a longer reaction time than 3-bromoanisole (Table 5, entries 8, 9). Furthermore, the reaction for styrene and *t*-butylacrylate were carried out in short times, but for acrylonitrile, the reaction takes longer time; because the olefins containing electron-withdrawing groups have less reactivity (entries 4, 5). Also, with regard to aryl chlorides, the reaction proceeded well in acceptable yields (entries 7, 16).

Finally, we provided a table which compared the presented conditions and catalytic activity of the catalyst in this study with other CN-type palladacycles reported in literature (Table 6). The results indicate that the prepared catalyst (**3**) has carried out the Heck reaction with highest yield in shortest reaction time and excellent recyclability relative to the other homogeneous and heterogeneous CN-type palladacycles.

3.3. Reusability of the catalyst

One of the most significant features of a heterogeneous catalyst is the recovery of the catalyst, especially from an industrial viewpoint. Hence, the recoverability of the catalyst was investigated via running the Heck reaction for iodobenzene and styrene under optimized conditions for several runs. At the end of the first run (after 1 h), the catalyst was isolated by centrifuging and after washing with dichloromethane and ethanol, it was dried at 80 °C. Then, it was applied for subsequent cycle. In this manner, the catalyst successfully carried out the reaction up to 8 cycles in high yields and its efficiency was not significantly decreased yet after 8 runs (Fig. 7). After removing of catalyst by centrifuging, the amount of leached palladium into the reaction solution was determined by ICP. The aforementioned investigation was performed

Table 5
Mizoroki–Heck reaction of aryl halides with various olefins^a.



| Entry | R ¹ | X | R ² | Product | Time (h) | Yield (%) ^b |
|-----------------|---------------------|----|--------------------|-----------|----------|------------------------|
| 1 ^c | 4-CN | Br | Ph | 6a | 1 | 95 |
| 2 | 4-CH ₃ | I | Ph | 6b | 1.5 | 90 |
| 3 | 4-COCH ₃ | I | Ph | 6c | 1.5 | 87 |
| 4 | 4-CH ₃ | I | CN | 6d | 10 | 85 |
| 5 | 4-COCH ₃ | I | CN | 6e | 10 | 83 |
| 6 ^c | 2-CH ₃ | Br | Ph | 6f | 1.5 | 90 |
| 7 ^c | 4-CN | Cl | Ph | 6g | 24 | 68 |
| 8 ^c | 4-OCH ₃ | Br | Ph | 6h | 4 | 82 |
| 9 ^c | 3-OCH ₃ | Br | Ph | 6i | 3 | 85 |
| 10 | 4-CH ₃ | I | CO ₂ Bu | 6j | 2 | 98 |
| 11 | 4-COCH ₃ | I | CO ₂ Bu | 6k | 2 | 96 |
| 12 ^c | 4-CH ₃ | Br | Ph | 6l | 1.5 | 91 |
| 13 ^c | 4-CN | Br | CO ₂ Bu | 6m | 12 | 90 |
| 14 | H | I | Ph | 6n | 1 | 98 |
| 15 ^c | H | Br | Ph | 6o | 1.5 | 85 |
| 16 ^c | 4-CN | Cl | CO ₂ Bu | 6p | 24 | 65 |
| 17 ^c | 3-OMe | Br | CO ₂ Bu | 6q | 3 | 86 |
| 18 | 3-CH ₃ | I | CO ₂ Bu | 6r | 1.5 | 93 |
| 19 | 3-CH ₃ | I | Ph | 6s | 1.5 | 92 |

^a Reaction conditions: aryl halide (1 mmol), olefine (1.2 mmol), Et₃N (1.5 mmol) and catalyst (**3**) (0.26 mol%) in DMF (3 mL) at 130 °C.

^b Isolated yields.

^c 0.75 mmol TBAB was added.

Table 6
Comparison of catalytic activity of various CN-type palladacycle based catalysts in the Mizoroki–Heck reaction^a.

| Entry | Catalyst | Pd (mol%) | Temp. (°C) | Time (h) | Yield (%) | Recyclability /Yield (%) | Ref. |
|-------|-----------------------------|-----------|------------|----------|-----------|--------------------------|------------|
| 1 | Imine-Pd | 0.064 | 100 | 12 | 100 | 1 | [33] |
| 2 | Fe-imine ^b -Pd | 0.0025 | 100 | 10 | 92 | 1 | [34] |
| 3 | Imine-Pd@PS ^c | 0.0064 | 140 | 11 | 100 | 3/100–0 | [33] |
| 4 | Imine-Pd@fluorous P | 0.02 | 100 | 5 | 85 | 4/85–52 | [43] |
| 5 | Oxime-Pd@PS | 0.1 | 120 | 6 | 94 | 4/94–88 | [47] |
| 6 | Fe-imine-Pd@CS ^d | 0.08 | 120 | 9 | 99 | 5/97–88 | [49] |
| 7 | Amine-Pd@PEG | 0.0045 | 100 | 16 | 80 | 4/80–76 | [50] |
| 8 | Hydrazone-Pd@ZnO | 0.26 | 130 | 1 | 98 | 8/98–85 | This study |

^a Iodobenzene and styrene have been considered as substrates.

^b Ferrocenyl imine.

^c Polystyrene.

^d Chitosan.

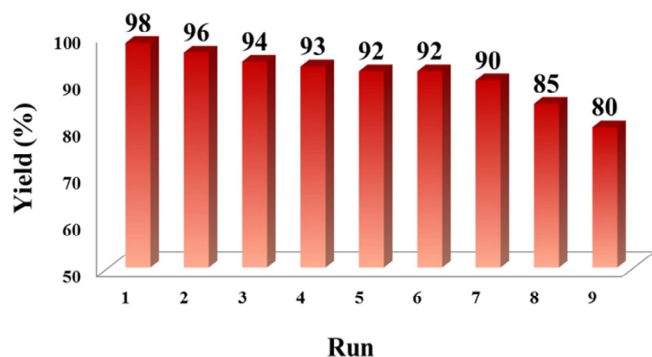


Fig. 7. Reusability of ZnO nanoplates supported hydrazone-based palladacycle as catalyst for Heck reaction; reaction conditions: iodobenzene (0.5 mmol), styrene (0.75 mmol), Et₃N (0.75 mmol) and 5 mg catalyst (0.26 mol%) in DMF (2 mL), at 130 °C for 1 h.

after the first and eight runs. The content of palladium leached into the solution was only 6.7×10^{-5} wt% (0.67 ppm) during the first reaction. Moreover, the amount of palladium in recovered catalyst after eight reaction runs was determined, which showed 0.43 wt% of total palladium has been released. Therefore, according to the result of leaching test, the prepared catalyst (**3**) is a highly effective heterogeneous catalyst to recover and reuse. Moreover, in order to prove the heterogeneity of the catalyst, a reaction was also performed under optimized condition in the presence of polyvinyl pyridine (PVPy) as poison (PVP is a strong poison for the homogeneous Pd species). The excess amount of PVPy was added at the beginning of reaction of iodobenzene with styrene. Then, the reaction was stopped after 1 h (according to the time for model reaction, Table 5, entry 14). The yield of isolated product (96%) showed insignificant decrease in reactivity of the catalyst which confirmed that no Pd nanoparticles was leached into the solution.

4. Conclusion

In a few words, we have been successful in preparation of a highly efficient and reusable heterogeneous ZnO nanoplates supported hydrazone-based palladacycle catalyst. This catalyst carried out the Mizoroki-Heck arylation of various olefins under air conditions with excellent yields for aryl iodides and bromides in short reaction times and also acceptable yields for aryl chlorides. Additionally, the catalyst is capable of being recovered and reused for eight sequential runs without considerable decrease in catalytic reactivity. Therefore, this approach provides a cost-effective synthetic method for preparation of stable palladacycles and makes the ZnO nanoplates supported hydrazone-based palladacycle complex appropriate for cross-coupling reactions.

Acknowledgement

We appreciatively acknowledge the Research Council of K.N. Toosi University of Technology for supporting this research.

Appendix A. Supplementary data

Supplementary data associated with this article can be found, in the online version, at <https://doi.org/10.1016/j.ica.2017.11.060>.

References

- [1] A. de Meijere, F. Diederich, *Metal-Catalyzed Cross-Coupling Reactions*, Wiley-VCH, New York, 2004.
- [2] J. Tsuji, *Palladium Reagents and Catalysts: New Perspectives for the 21st Century*, Wiley-VCH, New York, 2004.
- [3] J.P. Corbet, G. Mignani, *Chem. Rev.* 106 (2006) 651–710.
- [4] L.E. Overman, D.T. Ricca, V.D. Tran, *J. Am. Chem. Soc.* 115 (1993) 2042–2044.
- [5] L.F. Tietze, W. Ruhr, *Angew. Chem. Int. Ed.* 34 (1995) 1366–1368.
- [6] G. Ren, X. Cui, E. Yang, F. Yang, Y. Wu, *Tetrahedron* 66 (2010) 4022–4028.
- [7] R.B. Bedford, *Chem. Commun.* (2003) 1787–1796.
- [8] G.Y. Li, *J. Org. Chem.* 67 (2002) 3643–3650.
- [9] S.Y. Liu, M.J. Choi, G.C. Fu, *Chem. Commun.* (2001) 2408–2409.
- [10] O. Navarro, R.A. Kelly, S.P. Nolan, *J. Am. Chem. Soc.* 125 (2003) 16194–16195.
- [11] D. Badone, M. Baroni, R. Cardamone, A. Ielmini, U. Guzzi, *J. Org. Chem.* 62 (1997) 7170–7173.
- [12] C. Najera, J. Gil-Molto, S. Karlstroem, L.R. Falvello, *Org. Lett.* 5 (2003) 1451–1454.
- [13] S. Venkatraman, C.J. Li, *Org. Lett.* 1 (1999) 1133–1135.
- [14] J.F. Jensen, M. Johannsen, *Org. Lett.* 5 (2003) 3025–3028.
- [15] S.P. Nolan, *N-Heterocyclic Carbenes: Tools for Organometallic Synthesis*, Wiley-VCH, 2015.
- [16] J.L. Serrano, L. Garcia, I.J.S. Fairlamb, *Organometallics* 30 (2011) 5095–5109.
- [17] N. Seler, K.J. Szabo, *Chem. Rev.* 111 (2011) 2048–2076.
- [18] J. Dupont, C.S. Consorti, J. Spencer, *Chem. Rev.* 105 (2005) 2527–2571.
- [19] R. Ratti, *Can. Chem. Trans.* 2 (2014) 467–488.
- [20] W.A. Herrmann, K.O. Preysing, S.K. Schneider, *J. Organomet. Chem.* 687 (2003) 229–248.
- [21] M.E. Van der Boom, D. Milstein, *Chem. Rev.* 103 (2003) 1759–1792.
- [22] G. Dyker, *Chem. Ber. Recl.* 130 (1997) 1567–1578.
- [23] W.A. Herrmann, V.P.W. Böhm, C.P. Reisinger, *J. Organomet. Chem.* 576 (1999) 23–41.
- [24] A.D. Ryabov, *Synthesis* (1985) 233–252.
- [25] J. Dupont, M. Pfeffer, J. Spencer, *Eur. J. Inorg. Chem.* (2001) 1917–1927.
- [26] R.D. O'Sullivan, A.W. Parkins, *J. Chem. Soc. Chem. Commun.* (1984) 1165–1166.
- [27] J. Vicente, I. Saura-Llamas, P.G. Jones, *J. Chem. Soc. Dalton Trans.* (1993) 3619–3624.
- [28] R. Vanhelder, G. Verberg, *Recl. Trav. Chim. Pays-Bas* 84 (1965) 1263–1273.
- [29] I.R. Girling, D.A. Widdowson, *Tetrahedron Lett.* 23 (1982) 1957–1960.
- [30] D.A. Alonso, C. Najera, *Chem. Soc. Rev.* 39 (2010) 2891–2902.
- [31] T. Mino, Y. Shirae, M. Sakamoto, *J. Org. Chem.* 70 (2005) 2191–2194.
- [32] S. Iyer, A. Jayanthi, *Tetrahedron Lett.* 42 (2001) 7877–7878.
- [33] M. Nowotny, U. Hanefeld, H. Koningsveld, T. Maschmeyer, *Chem. Commun.* (2000) 1877–1878.
- [34] J.J. Hou, L.R. Yang, Y.J. Wu, *Chin. J. Chem.* 21 (2003) 717–719.
- [35] W.A. Herrmann, V.P.W. Böhm, *J. Organomet. Chem.* 572 (1999) 141–145.
- [36] N. Miyaura, *Metal-Catalyzed Cross-Coupling Reactions*, second ed., Wiley-VCH, Weinheim, 2004.
- [37] D. Villemin, D. Goussu, *Heterocycles* 29 (1989) 1255–1261.
- [38] S.B. Jang, *Tetrahedron Lett.* 38 (1997) 1793–1796.
- [39] F. Benvenuti, C. Carlini, M. Marchionna, A.M.R. Galletti, G. Sbrana, *J. Mol. Catal. A* 145 (1999) 221–228.
- [40] C.A. Parrish, S.L. Buchwald, *J. Org. Chem.* 66 (2001) 3820–3827.
- [41] K. Inada, L.R. Miyaura, *Tetrahedron* 56 (2000) 8661–8664.
- [42] C.A. McNamara, M.J. Dixon, M. Bradley, *Chem. Rev.* 102 (2002) 3275–3300.
- [43] C. Rocaboy, J.A. Gladysz, *New. J. Chem.* 27 (2003) 39–49.
- [44] M.G. Martinez, A. Baeza, D.A. Alonso, *Catalysts* 7 (2017) 94–110.
- [45] F.T. Luo, C.A. Lin, *Tetrahedron Lett.* 44 (2003) 7565–7568.
- [46] E. Alacid, C. Najera, *Synlett* (2006) 2959–2964.
- [47] E. Alacid, C. Najera, *ArKivoc* 8 (2008) 50–67.
- [48] E. Alacid, C. Najera, *Eur. J. Org. Chem.* (2008) 3102–3106.
- [49] Y. Yang, G. Li, Z. Song, P. Liu, *Lett. Org. Chem.* 7 (2010) 533–538.
- [50] K. Karami, Z. Karami-Moghadam, M. Hosseini-Kharat, *Catal. Commun.* 43 (2014) 25–28.
- [51] M. Gholinejad, M. Razeghi, C. Najera, in: *RSC Adv.* 5 (2015) 49568–49576.
- [52] C. Baleizao, A. Corma, H. Garcia, A. Leyva, *J. Org. Chem.* 69 (2004) 439–446.
- [53] K. Mennecke, W. Solodenko, A. Kirschning, *Synthesis* (2008) 1589–1599.
- [54] M.D. Liedekerke, *Ullmann's Encyclopedia of Industrial Chemistry*, Wiley-VCH, Weinheim, 2006.
- [55] D. Segets, J. Gradl, R.K. Taylor, V. Vassilev, W. Peukert, *ACS Nano* 3 (2009) 1703–1710.
- [56] U. Ozgur, Y.L. Alivov, C. Liu, A. Teke, M.A. Reshchikov, S. Dogan, V. Avrutin, *J. Appl. Phys.* 98 (2005) 1–103.
- [57] S. Bhattacharyya, A. Gedanken, *Microporous Mesoporous Mater.* 110 (2007) 553–559.
- [58] B. Ludi, M. Niederberger, *Dalton Trans.* 42 (2013) 12554–12568.
- [59] C.W. Lim, S. Lee, *Nano Today* 5 (2010) 412–434.
- [60] S. Shylesh, V. Schunemann, W.R. Thiel, *Angew. Chem. Int. Ed.* 49 (2010) 3428–3459.
- [61] T. Zeng, W.W. Chen, C.M. Cirtiu, A. Moores, G. Song, C.J. Li, *Green Chem.* 12 (2010) 570–573.
- [62] D. Zhang, C. Zhou, Z. Sun, L.Z. Wu, C.H. Tunga, T. Zhang, *Nanoscale* 4 (2012) 6244–6255.
- [63] S. Rostamizadeh, M. Rezghi, N. Shadjou, M. Hasanzadeh, *J. Chin. Chem. Soc.* 60 (2013) 1317–1322.
- [64] S. Rostamizadeh, M. Nojavan, R. Aryan, E. Isapoor, M. Azad, *J. Mol. Catal. A* 374 (2013) 102–110.
- [65] S. Rostamizadeh, N. Zekri, L. Tahershamsi, *Polycycl. Aromat. Compd.* 34 (2014) 542–560.
- [66] F. Nouri, S. Rostamizadeh, M. Azad, *Mol. Catal.* 443 (2017) 286–293.
- [67] Z.R. Tian, J.A. Voigt, J. Liu, *Nat. Mater.* 2 (2003) 821–826.
- [68] Q. Zhou, W. Chen, L. Xu, *Sensors* 13 (2013) 6171–6182.
- [69] A. Pramanik, S. Das, K. Dutta, *CrystEngComm* 15 (2013) 6349–6358.
- [70] M.H. Jung, M.J. Chu, *J. Mater. Chem.* 2 (2014) 6675–6682.
- [71] J. Safari, S. Gandomi-Ravandi, *Synth. Commun.* 41 (2011) 645–651.
- [72] K. Kaneko, *J. Membr. Sci.* 96 (1994) 59–89.
- [73] J. Horniakova, T. Raja, Y. Kubota, Y. Sugi, *J. Mol. Catal. A* 217 (2004) 73–80.
- [74] Z. Jing, J. Zhan, *Adv. Mater.* 20 (2008) 4547–4551.
- [75] E.S. Jang, *J. Korean Chem. Soc.* 54 (2017) 167–183.
- [76] S.G. Leonardi, *Chemosensors* 5 (2017) 17–45.
- [77] K.S.W. Sing, *Pure Appl. Chem.* 54 (1982) 2201–2218.
- [78] M. Brun, A. Berthet, J.C. Bertolini, *J. Electron. Spectrosc. Rel. Phenom.* 104 (1999) 55–60.
- [79] L. Huang, Y. Wang, Z. Wang, F. Chen, J. Tan, P.K. Wong, *Phys. Chem.* 2 (2012) 27–34.
- [80] M. Salavati-Niasari, M. Bazarganipour, *Appl. Surf. Sci.* 255 (2008) 2963–2970.
- [81] F. Bellina, C. Chiappe, *Molecules* 15 (2010) 2211–2245.
- [82] B.K. Allam, K.N. Singh, *Synthesis* (2011) 1125–1131.
- [83] D.H. Lee, A. Taher, S. Hossain, M.J. Jin, *Org. Lett.* 13 (2011) 5540–5543.